

Molecular Recognition of Sialyl Lewis^x and Related Saccharides by Two Lectins

Thomas Haselhorst, Thomas Weimar, and Thomas Peters*

Contribution from the Institut für Chemie, Medizinische Universität zu Lübeck, Ratzeburger Allee 160, D-23538 Lübeck, Germany

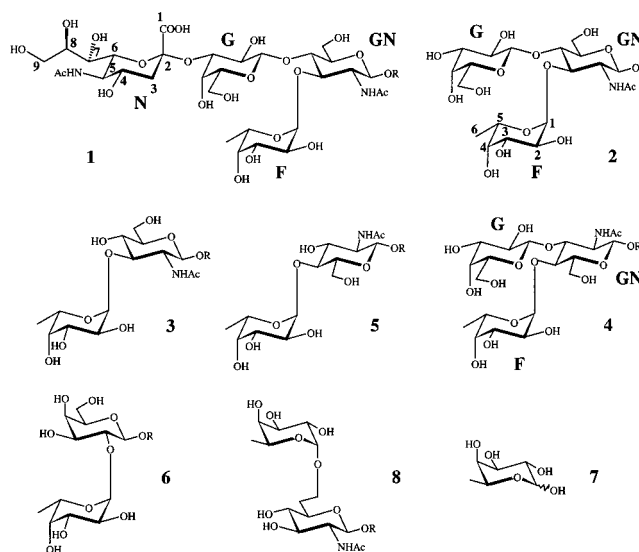
Received May 9, 2001. Revised Manuscript Received July 13, 2001

Abstract: The interaction of sialyl Lewis^x, Lewis^x, and α -L-Fuc-(1 \rightarrow 3)- β -D-GlcNAc with isolectin A from *Lotus tetragonolobus* (LTL-A), and with *Aleuria aurantia* agglutinin (AAA) was studied using NMR experiments and surface plasmon resonance. Both lectins are specific for fucose residues. From NMR experiments it was concluded that α -L-Fuc-(1 \rightarrow 3)- β -D-GlcNAc and Lewis^x bound to both lectins, whereas sialyl Lewis^x only bound to AAA. Increased line broadening of ¹H NMR signals of the carbohydrate ligands upon binding to AAA and LTL-A suggested that AAA bound to the ligands more tightly. Further comparison of line widths showed that for both lectins binding strengths decreased from α -L-Fuc-(1 \rightarrow 3)- β -D-GlcNAc to Lewis^x and were lowest for sialyl Lewis^x. Surface plasmon resonance measurements were then employed to yield accurate dissociation constants. TrNOESY, QUIET-trNOESY, and trROESY experiments delivered bioactive conformations of the carbohydrate ligands, and STD NMR experiments allowed a precise epitope mapping of the carbohydrates bound to the lectins. The bioactive conformation of Lewis^x bound to LTL-A, or AAA revealed an unusual orientation of the fucose residue, with negative values for both dihedral angles, ϕ and ψ , at the α (1 \rightarrow 3)-glycosidic linkage. A similar distortion of the fucose orientation was also observed for sialyl Lewis^x bound to AAA. From STD NMR experiments it followed that only the L-fucose residues are in intimate contact with the protein. Presumably steric interactions are responsible for locking the sialic acid residue of sialyl Lewis^x in one out of many orientations that are present in aqueous solution. The sialic acid residue of sialyl Lewis^x bound to AAA adopts an orientation similar to that in the corresponding sialyl Lewis^x/E-selectin complex.

Introduction

Carbohydrate–protein interactions are key events in a variety of cell–cell interactions.¹ Therefore, strategies have been explored to develop drugs that mimic carbohydrate epitopes responsible for such specific interactions² to potentially cure associated disease states, including cancer. For instance, it has been shown that in human lung and colon carcinomas highly metastatic tumor cells express more sialyl Lewis^x epitopes (sLe^x, α -D-Neu5Ac-(2 \rightarrow 3)- β -D-Gal-(1 \rightarrow 4)-[α -L-Fuc(1 \rightarrow 3)]- β -D-GlcNAc-Ome, **1**; see Chart 1) on the surface and bind more strongly to E-selectin than their poorly metastatic counterparts.³ Nevertheless, no direct evidence is yet available that E-selectin is the functional receptor responsible for such metastatic processes. Therefore, the binding of sLe^x to other proteins certainly is of considerable biological interest. To perform a rational design of carbohydrate-based drugs knowledge is required about the bioactive conformation of natural carbohydrate ligands in the protein-bound state. Hence, we studied the interaction of

Chart 1. Chemical Formulas, Numbering Conventions, and Abbreviations of the Oligosaccharides Investigated^a



^a Key: **1**, sialyl Lewis^x, sLe^x, R = -(CH₂)₈-COOMe; **2**, Lewis^x, Le^x, R = Me; **3**, α -L-Fuc-(1 \rightarrow 3)- β -D-GlcNAc, R = Me; **4**, Lewis^a, Le^a, R = Me; **5**, α -L-Fuc-(1 \rightarrow 4)- β -D-GlcNAc, R = Me; **6**, α -L-Fuc-(1 \rightarrow 2)- β -D-Gal, R = Me; **7**, L-fucose; **8**, α -L-Fuc-(1 \rightarrow 6)- β -D-GlcNAc, R = Me. Abbreviations for the pyranose residues are as follows: GN = GlcNAc, N-acetylglucosamine; G = Gal, galactose; F = Fuc, fucose; N = Neu5Ac, neuramic acid.

synthetic sLe^x (**1**), the constituent trisaccharide Le^x (**2**) (Lewis^x, β -D-Gal-(1 \rightarrow 4)[α -L-Fuc-(1 \rightarrow 3)]- β -D-GlcNAc-OMe), and the

* Corresponding author. Tel.: +49-451-500-4230. Fax: +49-451-500-4241. E-mail: thomas.peters@chemie.mu-luebeck.de.

(1) (a) Rudd, P. M.; Elliott, T.; Cresswell, P.; Wilson, I. A.; Dwek, R. A. *Science* **2001**, *291*, 2370–2376. (b) Helenius, A.; Aebi, M. *Science* **2001**, *291*, 2364–2369.

(2) (a) Sears, P.; Wong, C.-H. *Science* **2001**, *291*, 2344–2350. (b) Bertozzi, C. R.; Kiessling, L. L. *Science* **2001**, *291*, 2357–2364. (c) Kitov, P. I.; Sadowska, J. M.; Mulvey, G.; Armstrong, G. D.; Ling, H.; Pannu, N. S.; Read, R. J.; Bundle, D. R. *Nature* **2000**, *403*, 669–672. (d) Schweizer, F.; Hinds Gaul, O. *Curr. Opin. Chem. Biol.* **1999**, *3*, 291–298. (e) Ernst, B.; Oehrlin, R. *Glycoconj. J.* **1999**, *16*, 161–170.

(3) (a) Fukuda, M. N.; Ohya, C.; Lowitz, K.; Matsuo, O.; Pasqualini, R.; Ruoslahti, E.; Fukuda, M. *Cancer Res.* **2000**, *60*, 450–456. (b) Ohya, C.; Tsuboi, S.; Fukuda, M. *EMBO J.* **1999**, *18*, 1516–1525.

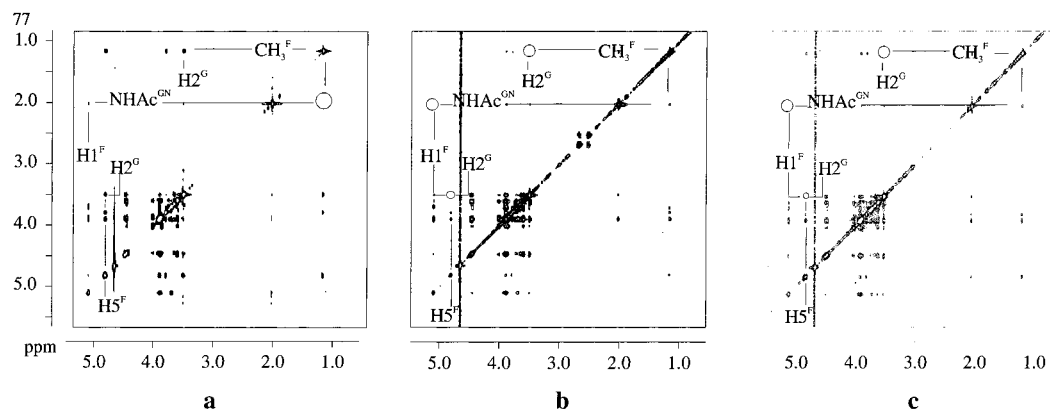


Figure 1. NOESY and trNOESY spectra of Le^x (**2**) (310 K, 500 MHz): (a) aqueous solution without lectin present; (b) in the presence of AAA; (c) in the presence of LTL-A. Mixing times were (a) 900 ms and (b, c) 150 ms. Cross-peaks in spectrum a are negative (opposite sign as the diagonal peaks), and cross-peaks in spectra b and c are positive (same sign as the diagonal peaks). The strong diagonal and off-diagonal peaks at ca. 2.5 ppm originate from the protein sample and are not due to the ligand.

disaccharide α -L-Fuc-(1 \rightarrow 3)- β -D-GlcNAc-OMe (**3**) with two lectins, *Lotus tetragonolobus* isolectin A (LTL-A)⁴ and *Aleuria aurantia* agglutinin (AAA).⁵ Previously, we and others have devoted much attention to the analysis of the bioactive conformation of sLe^x bound to E-selectin using NMR experiments.⁶ Although the various models of sLe^x bound to E-selectin differ in details, they correspond in their gross conformational features. The α (2 \rightarrow 3)-linkage between neuramic acid and galactose is fixed in an orientation which is significantly populated in aqueous solution, and the Le^x trisaccharide core is rather similar to its conformation in aqueous solution. The principal purpose of the present study is to analyze sLe^x and Le^x bound to other receptor proteins than E-selectin and to explore the space of their potential protein-bound conformations.

Results

Conformational Analysis of Saccharides 1–3. A complete assignment of ^1H NMR resonance signals was achieved on the basis of COSY, TOCSY, and NOESY experiments (available from the Supporting Information). Chemical shifts of the saccharides were in accordance with values reported previously.^{6,7} For the conformational analysis of tetrasaccharide **1** the reader is referred to the literature. For trisaccharide **2**, however, an interglycosidic NOE was observed that had not

(4) (a) Cheng, W.; Bullitt, E.; Bhattacharyya, L.; Brewer, C. F.; Makowski, L. *J. Biol. Chem.* **1998**, *273*, 35016–35022. (b) Yan, L.; Wilkins, P. P.; Alvarez-Manilla, G.; Do, S. I.; Smith, D. F.; Cummings, R. D. *Glycoconj. J.* **1997**, *14*, 45–55. (c) Konami, Y.; Yamamoto, K.; Osawa, T. *FEBS Lett.* **1990**, *268*, 281–286. (d) Pereira, M. E.; Kabat, E. A. *Biochemistry* **1974**, *16*, 13, 3184–3192. (e) Kalb, A. J. *Biochim. Biophys. Acta* **1968**, *168*, 532–536. (f) Yarif, J.; Kalb, A. J.; Katchalski, E. *Nature* **1967**, *215*, 890–891.

(5) (a) Nagata, Y.; Fukumori, F.; Sakai, H.; Hagiwara, T.; Hiratsuka, Y.; Kochibe, N.; Kobata, A. *Biochim. Biophys. Acta* **1991**, *1076*, 187–90. (b) Yazawa, S.; Kochibe, N.; Asao, T. *Immunol. Invest.* **1990**, *19*, 319–27. (c) Fukumori, F.; Takeuchi, N.; Hagiwara, T.; Ohbayashi, H.; Endo, T.; Kochibe, N.; Nagata, Y.; Kobata, A. *J. Biochem.* **1990**, *107*, 190–196. (d) Fukumori, F.; Takeuchi, N.; Hagiwara, T.; Ito, K.; Kochibe, N.; Kobata, A.; Nagata, Y. *FEBS Lett.* **1989**, *250*, 153–156. (e) Debray, H.; Montreuil, J. *Carbohydr. Res.* **1989**, *185*, 15–26. (f) Kochibe, N.; Furukawa, K. *Biochemistry* **1980**, *19*, 2841–2846.

(6) (a) Harris, R.; Kiddle, G. R.; Field, R. A.; Ernst, B.; Magnani, J. L.; Homans, S. W. *J. Am. Chem. Soc.* **1999**, *121*, 2546. (b) Scheffler, K.; Brisson, J.-R.; Weisemann, R.; Magnani, J. L.; Wang, W. T.; Ernst, B.; Peters, T. *J. Biomol. NMR* **1997**, *9*, 423–436. (c) Poppe, L.; Brown, G. S.; Philo, J. S.; Nikrad, P. V.; Shah, B. H. *J. Am. Chem. Soc.* **1997**, *119*, 1727–1736. (d) Scheffler, K.; Ernst, B.; Katopodis, A.; Magnani, J. L.; Wang, W. T.; Weisemann, R.; Peters, T. *Angew. Chem., Int. Ed. Engl.* **1995**, *34*, 1841–1844; *Angew. Chem.* **1995**, *107*, 2034–2037. (e) Cooke, R. M.; Hale, R. S.; Lister, S. G.; Shah, G.; Weir, M. P. *Biochemistry* **1994**, *33*, 10591–10596.

Table 1. Dihedral Angles for the Global and Local Minimum Conformations of Le^x ^a

min	ϕ/ψ (deg)		rel energy (kcal/mol)
	Gal(1 \rightarrow 4)GlcNAc	Fuc(1 \rightarrow 3)GlcNAc	
A	52/10	48/26	0.0
B	67/17	–25/–28	7.3
C	64/22	27/–179	11.1
D	40/23	7/5	8.3

^a The values were calculated using the program GEGOP.

been described previously. All NOEs of **2** were positive at 310 K and 500 MHz. NOESY spectra of **2** revealed the following interglycosidic NOEs: $\text{H1}^{\text{F}}-\text{NHAc}^{\text{GN}}$, $\text{H5}^{\text{F}}-\text{H2}^{\text{G}}$, $\text{CH}_3^{\text{F}}-\text{H2}^{\text{G}}$, and $\text{H1}^{\text{F}}-\text{H2}^{\text{G}}$ (Figure 1). Except for the weak NOE $\text{H1}^{\text{F}}-\text{H2}^{\text{G}}$ these NOEs had been reported before. Metropolis Monte Carlo (MMC) simulations⁸ were then performed to relate the experimental data to a conformational model that includes motional averaging. In accordance with previous calculations a global minimum A was identified (Table 1). A local minimum B which is characterized by negative dihedral angles at the α (1 \rightarrow 3)-glycosidic linkage between fucose and *N*-acetylglucosamine has been predicted by other authors but so far has not been experimentally verified.⁹ It is this local minimum that accounts for the interglycosidic NOE $\text{H1}^{\text{F}}-\text{H2}^{\text{G}}$. In the global minimum A the galactose and the fucose residues display a stacked arrangement giving rise to characteristic interglycosidic NOEs, $\text{H1}^{\text{F}}-\text{NHAc}^{\text{GN}}$, $\text{H5}^{\text{F}}-\text{H2}^{\text{G}}$, and $\text{H6}^{\text{F}}-\text{H2}^{\text{G}}$. In the local minimum B the orientation of the two pyranose rings is distorted such that the distance $\text{H5}^{\text{F}}-\text{H2}^{\text{G}}$ becomes large (>5 Å) and the distance $\text{H1}^{\text{F}}-\text{H2}^{\text{G}}$ smaller (<3 Å) (Figure 2). Therefore, we conclude that the conformational properties of trisaccharide **1** in aqueous solution are described by a model where two

(7) (a) Berthault, P.; Birlirakis, N.; Rubinstenn, G.; Sinay, P.; Desvaux, H. *J. Biomol. NMR* **1996**, *8*, 23–35. (b) Rutherford, T. J.; Spackman, D. G.; Simpson, P. J.; Homans, S. W. *Glycobiology* **1994**, *4*, 59–68. (c) Mukhopadhyay, C.; Miller, K. E.; Bush, C. A. *Biopolymers* **1994**, *34*, 21–29. (d) Miller, K. E.; Mukhopadhyay, C.; Cagas, P.; Bush, A. C. *Biochemistry* **1992**, *31*, 6703–6709. (e) Ichikawa, Y.; Lin, Y. C.; Dumas, D. P.; Shen, G.-J.; Garcia-Junceda, E.; Williams, M. A.; Bayer, R.; Ketcham, C.; Walker, L. E.; Paulson, J. C.; Wong, C.-H. *J. Am. Chem. Soc.* **1992**, *114*, 9283–9289. (f) Wormald, M. R.; Edge, C. J.; Dwek, R. A. *Biochem. Biophys. Res. Commun.* **1991**, *180*, 1214–1221.

(8) (a) Peters, T.; Meyer, B.; Stuike-Prill, R.; Somorjai, R.; Brisson, J.-R. *Carbohydr. Res.* **1993**, *238*, 49–73. (b) Stuike-Prill, R.; Meyer, B. *Eur. J. Biochem.* **1991**, *194*, 903–919.

(9) (a) Poveda, A.; Asensio, J. L.; Martín-Pastor, M.; Jiménez-Barbero, J. *J. Biomol. NMR* **1997**, *10*, 29–43. (b) Lommerse, J. P. M.; Kroon-Batenburg, L. M. J.; Kroon, J.; Kamerling, J. P.; Vliegthart, J. F. G. *J. Biomol. NMR* **1995**, *5*, 79–94.

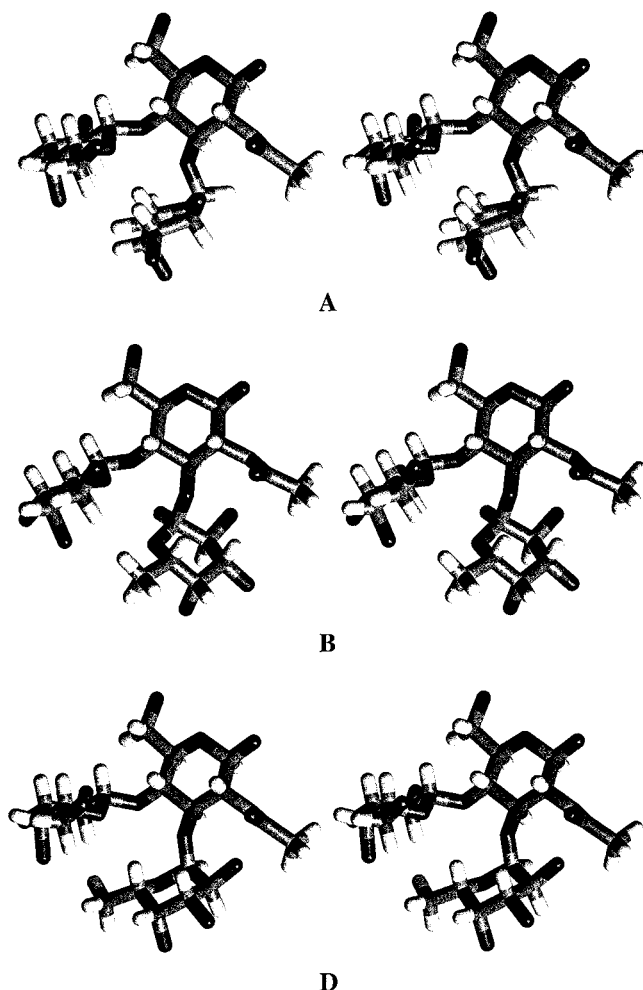


Figure 2. Stereopictures (relaxed eye) of the global minimum A and local minima B and D of trisaccharide Le^x (**2**). In the global minimum A, the galactose and the fucose residue show a stacking interaction. In minima B and D this stacking interaction is removed, and the hydrophobic side of Le^x can interact with the lectin binding site. Minimum B is recognized by AAA, and minimum D is recognized by LTL-A (cf. Table 1).

conformational families are present. One of the families is characterized by the global minimum A, and the other family is represented by the local minimum B, which is populated to a rather small percentage (<1–5%).

The experimental data do not support the presence of the local minimum C (Table 1), which would be characterized by a rather short distance between H6^F and NAc^{GN} (~2 Å). A corresponding interglycosidic NOE was not observed.

For disaccharide **3** the NOE data support the notion that one main conformational family similar to the global minimum A adequately describes the conformational properties of this compound. However, it should be mentioned that a small percentage of conformations similar to B would not be detectable from NOESY experiments because no specific interglycosidic NOEs would occur.

Conformation of the Le^x Trisaccharide Bound to AAA. Addition of AAA to an aqueous solution of **2** led to the observation of strong negative trNOEs. The trNOESY spectrum of trisaccharide **2** in the presence of AAA showed a significantly different trNOESY cross-peak pattern as compared to the NOESY spectrum of **2** in aqueous solution (Figure 1). Three of the most prominent interglycosidic NOEs, i.e., H1^F–NHA^{GN}, H5^F–H2^G, and H6^F–H2^G, had disappeared from the

trNOESY spectrum. Instead, the interglycosidic trNOE H1^F–H2^G had gained intensity (Figure 1). Another weak interglycosidic trNOE was observed between the fucose methyl group H6^F and H6^G (see Supporting Information). Additionally, the cross-peak between the *N*-acetyl group of GlcNAc and the signals around 3.88 ppm gained significant intensity in the trNOESY spectrum. This could be due to a close contact between H3^F and NAc^{GN}. Unfortunately, H3^F, H3^{GN}, and H2^{GN} had almost identical chemical shifts, and therefore, an unambiguous assignment was difficult. The disappearance of characteristic trNOEs and the observation of trNOEs H1^F–H2^G and H6^F–H6^G were incompatible with global minimum A as the bound conformation. This indicates that the α(1→3)-glycosidic linkage undergoes a major conformational change upon binding to AAA, and therefore, the global minimum A is not the one that is recognized by the lectin. On the other hand, the trNOEs observed across the β(1→4)-glycosidic linkage between the Gal and the GlcNAc residues correspond largely to the NOEs observed for the free Le^x trisaccharide **2**, indicating that this glycosidic linkage is less affected upon binding to the protein.

Since the interglycosidic trNOE H1^F–H2^G is weak, and since it is well documented that spin diffusion can lead to false distance constraints when generating a bioactive conformation of a ligand, we performed trROESY and QUIET-trNOESY¹⁰ experiments as this has been described in detail before.¹¹ The trNOE H1^F–H2^G was present in all spectra verifying that it was not generated by spin diffusion via protein protons.

Very weak interglycosidic trNOEs H1^F–H5^{GN} and H1^F–H1^G were found to be due to spin diffusion, since they disappeared in trROESY spectra. Another weak trNOE between the fucose C6-methyl group H6^F and the *N*-acetyl group NAc^{GN} of the *N*-acetylglucosamine residue was also scrutinized since the presence of this interglycosidic trNOE would indicate an anti-conformation (local minimum C, Table 1) at the α(1→3)-glycosidic linkage. The trNOESY, trROESY, and QUIET-trNOESY spectrum are displayed in Figure 3 clearly demonstrating that the presence of the cross-peak H6^F–NAc^{GN} is due to spin diffusion. In the trROESY spectrum no cross-peak was observed, and in the QUIET-trNOESY spectrum, only a rather small residual peak was left that was probably due to imperfect inversion of the band selective 180° I-BURP pulse in the center of the mixing time or to relaxation processes during the duration of the I-BURP pulse.

On the basis of QUIET-trNOESY buildup curves (available as Supporting Information) the conformation of Le^x bound to AAA was calculated. A MMC simulation of the trisaccharide Le^x with the temperature parameter set at 2000 K was performed to generate a most complete ensemble of conformations. Distance constraints were derived from the buildup curves and, subsequently, used as a filter to select the subset of conformations that represents the bound conformation following the protocols described previously.¹¹ Table 2 summarizes the distance constraints that were applied. Population distribution plots were calculated to visualize the results (Figure 4). The population distributions that were generated by applying distance constraints gave a measure for the experimental error with which a bioactive conformation can be determined. It was found that the local minimum B (Table 1) represented the conformation of Le^x bound to AAA quite well.

(10) Vincent, S. J. F.; Zwahlen, C.; Post, C. B.; Burgner, J. W.; Bodenhausen, G. *Proc. Natl. Acad. Sci. U.S.A.* **1997**, *94*, 4383–4388.

(11) (a) Maaheimo, H.; Kosma, P.; Brade, L.; Brade, H.; Peters, T. *Biochemistry* **2000**, *39*, 12778–12788. (b) Haselhorst, T.; Espinosa, J.-F.; Jiménez-Barbero, Sokolowski, T.; Kosma, P.; Brade, H.; Brade, L.; Peters, T. *Biochemistry* **1999**, *38*, 6449–6459.

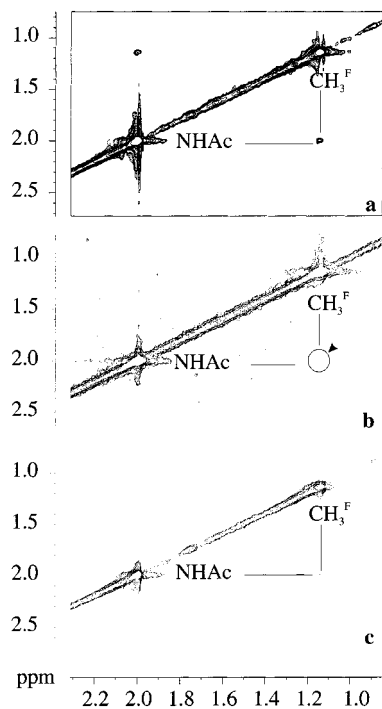


Figure 3. (a) trNOESY, (b) trROESY, and (c) QUIET trNOESY spectrum of **2** in the presence of AAA. The QUIET-trNOESY experiment was recorded with a 5 ms band-selective I-BURP inversion pulse (inversion of regions 2.60–0.60 ppm). The mixing time was 150 ms for all experiments. The trNOE cross-peak that is present in the trNOESY spectrum a is due to spin diffusion because it is absent in the trROESY spectrum c. In the QUIET-trNOESY spectrum the cross-peak has a largely reduced intensity. The residual intensity is probably due to imperfect inversion properties of the I-BURP pulse or to concomitant inversion of alkyl amino acid side chains leading to minor spin diffusion via the protein.

Table 2. Distance Restraints from trNOESY or QUIET-trNOESY Spectra for Le^x Bound to AAA and to LTL-A^a

restraints	positive/negative	dists (Å)	r_1 – r_u (Å)
AAA			
H5 ^F –H4 ^F	positive	2.36	1.89–2.83
H5 ^F –H3 ^F		2.17	1.74–2.60
H1 ^F –H3 ^{GN}		1.85	1.48–2.22
H1 ^G –H6 ^p S ^{GN}		2.23	1.78–2.68
H1 ^F –H2 ^G		3.15	2.52–3.78
H1 ^G –H4 ^{GN}		2.50 ^b	2.00–3.00
H6 ^F –H6 ^p S ^G		3.00 ^b	2.50–3.50
H6 ^F –H6 ^p R ^G		3.00 ^b	2.50–3.50
H5 ^F –H2 ^G	negative		>4.0
H1 ^F –NHAc			>4.0
H6 ^F –H2 ^G			>4.0
LTL-A			
H5 ^F –H4 ^F	positive	2.36	1.89–2.83
H5 ^F –H3 ^F		2.11	1.69–2.53
H1 ^F –H3 ^{GN}		1.85	1.48–2.22
H1 ^G –H6 ^p S ^{GN}		2.27	1.96–2.95
H1 ^G –H4 ^{GN}		2.50 ^b	2.00–3.00
H5 ^F –H2 ^G	negative		>4.0
H1 ^F –NHAc			>4.0
H6 ^F –H2 ^G			>4.0

^a Distances were obtained using the ISPA approximation with the distance between H5^F and H4^F serving as a reference (2.36 Å). A positive restraint corresponds to an observed trNOE. A negative restraint corresponds to a trNOE that is not observed. For negative constraints a cutoff distance of 4.0 Å instead of a more usual value around 5.5 Å was used to allow for a more generous error margin. r_1 and r_u denote lower and upper distance constraints, respectively. ^b For these trNOEs no accurate integration was possible and the values were estimated.

Conformation of the Le^x Trisaccharide Bound to LTL-A. Addition of LTL-A to an aqueous solution of the Le^x

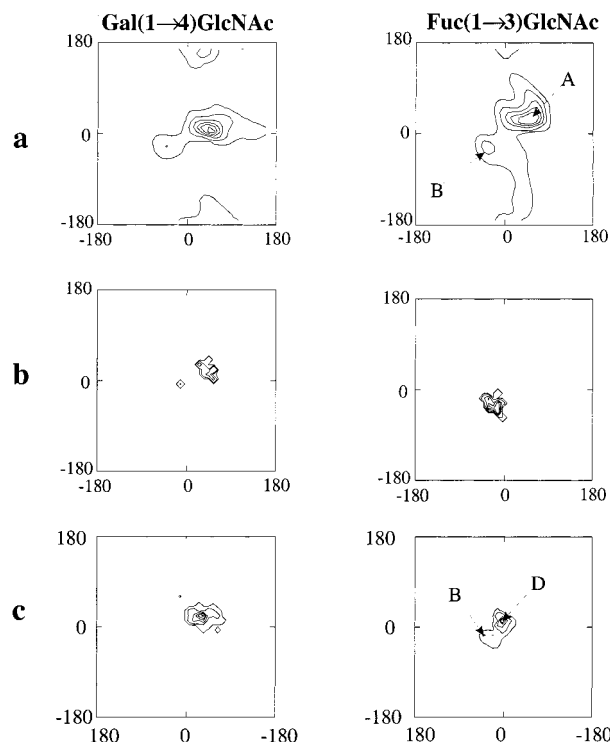


Figure 4. Contour plots showing the relative population of conformational space around the β -D-Gal(1 \rightarrow 4)- β -D-GlcNAc and the α -L-Fuc(1 \rightarrow 3)- β -D-GlcNAc-glycosidic linkage in **2**. The ϕ/ψ maps of each glycosidic linkage were divided into bins of 10° in the ϕ and ψ directions, and the number of conformations in each bin was counted. Then, contour levels were calculated relative to the highest populated bin (global minimum). The contour levels from outside to inside are 1–10%, 10–30%, 30–50%, 50–70%, 70–90%, and more than 90% of the number of conformations in the most populated bin.^{11a} Key: (a) MMC simulation at 2000 K; (b) Le^x trisaccharide **2** bound to AAA; (c) Le^x trisaccharide **2** bound to LTL-A. The contour plots in (b) and (c) were derived from the MMC simulation in (a) by applying the distance constraints from Table 2 as a filter.

trisaccharide **2** led to trNOESY spectra similar to the ones obtained for Le^x in the presence of AAA (Figure 1). Therefore, only effects that differ from the above case will be addressed in the following. In general, the trNOEs were weaker suggesting that the binding affinity of **2** to LTL-A was lower than toward AAA (compare the trNOE buildup curves available from the Supporting Information). As this had been described above, trROESY and QUIET-trNOESY experiments were applied to test for spin diffusion. From these experiments it became clear that there were differences in the binding modes of Le^x bound to LTL-A and AAA. The interglycosidic trNOE H6^F–H6^G was not observed at all (see Supporting Information), and the interglycosidic trNOE H1^F–H2^G was found to disappear in trROESY as well as in QUIET-trNOESY spectra. Therefore, we assigned the cross-peak between H1^F and H2^G to be due to spin diffusion and did not include it in the distance constraints to generate the bound conformation.

A list of distance constraints (Table 2) was derived from the QUIET-trNOE buildup curves and led to the ensemble of conformations that is shown in the population distribution plot in Figure 4. Obviously, the exclusion of the H1^F–H2^G distance constraints allowed the α (1 \rightarrow 3)-glycosidic linkage to adopt a conformation with dihedral angles ϕ and ψ close to zero, termed conformation D (Table 1). From the contour plots (Figure 4) conformations similar to the local minimum B were also identified as possible bound conformations because the distance H1^F–H2^G was not included as a negative constraint. Inclusion

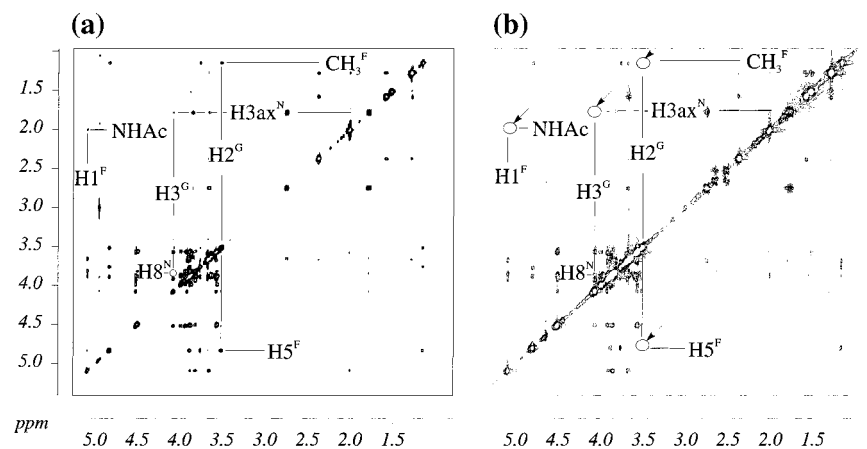


Figure 5. NOESY and trNOESY spectra of sLe^x (**2**): (a) in aqueous solution (303 K, 600 MHz, mixing time 1 s); (b) in the presence of AAA (310 K, 500 MHz, mixing time 350 ms).

Table 3. Distance Restraints from trNOESY Spectra for SLe^x Bound to AAA^a

restraints	positive/negative	dists (Å)	r_1 – r_u (Å)
H1 ^F –H3 ^{GN}	positive	2.03	1.87–2.80
H1 ^G –H4 ^{GN}		3.00 ^b	2.50–3.50
H3 ^G –H8 ^N		2.83	2.27–3.40
H1 ^F –NHAc ^{GN}	negative		>4.0
H5 ^F –H2 ^G			>4.0
CH ₃ ^F –H2 ^G			>4.0
H3 ^G –H3ax ^N			>4.0
H3 ^G –H3eq ^N			>4.0

^a Distances were obtained using the ISPA approximation with the distance between H5^F and H4^F serving as a reference (2.36 Å). A positive restraint corresponds to an observed trNOE. A negative restraint corresponds to a trNOE that is not observed. r_1 and r_u denote lower and upper distance constraints, respectively. ^bFor these trNOEs no accurate integration was possible and the values were estimated.

of this latter restraint only left the region around conformation D. We conclude that in the case of Le^x binding to LTL-A a bioactive conformation D is adopted.

Conformation of the sLe^x Tetrasaccharide Bound to AAA. trNOEs that were observed upon addition of AAA to an aqueous solution of sLe^x tetrasaccharide **1** were of lower absolute intensity than those observed for the corresponding Le^x trisaccharide **2** binding to AAA. This was an indication that the binding affinity of tetrasaccharide **1** to AAA was lower than that of trisaccharide **2** to AAA. For the Le^x trisaccharide part of sLe^x the overall pattern of trNOEs was almost identical to that of Le^x in the presence of AAA and LTL-A (Figure 5). As observed for the binding of Le^x to LTL-A, the trNOEs H1^F–H2^G, H1^F–H5^{GN}, and H1^F–H1^G were identified as spin-diffusion effects by utilizing trROESY experiments and were therefore not used as distance constraints for the determination of the bioactive conformation of sLe^x bound to AAA.

For the α(2→3)-glycosidic linkage between Neu5Ac and Gal, trNOEs differed from the NOEs observed for free sLe^x (Figure 5). An interglycosidic NOE between H3^G and H3_{ax}^N was not observed in the trNOESY spectrum. At the same time, a trNOE was observed between H3^G and H8^N not present in the NOESY spectrum of free sLe^x. The same effects had been observed before for the binding of sLe^x to E-selectin and had been a key to determine the conformation of sLe^x bound to E-selectin.⁶

As described above, distance constraints were derived from the trNOESY spectra (Table 3) and were then used to extract the bioactive conformation of sLe^x from a MMC simulation. The analysis showed that the orientation of the neuramic acid relative to the galactose residue was almost identical to the

orientation observed for sLe^x bound to E-selectin, called conformation “a” in the following, to discriminate between the α(1→3)- and the α(2→3)-linkage (Table 4). For the α(1→3)-glycosidic linkage between Fuc and GlcNAc either an orientation corresponding to conformation B found for Le^x bound to AAA (Table 1) or an orientation similar to conformation D found for Le^x bound to LTL-A was possible when the trNOE H1^F–H2^G was not included as a negative distance constraint. With an additional negative distance constraint for the distance H1^F–H2^G, only the orientation corresponding to conformation D was possible. Therefore, we conclude that the conformation of sLe^x bound to AAA corresponds to conformation aD in Table 4. The bioactive conformation of sLe^x is shown in Figure 10.

No trNOEs were observed for sLe^x in the presence of LTL-A suggesting that the tetrasaccharide is not bound by the lectin.

Conformation of Disaccharide 3 Bound to AAA and LTL-A. trNOE effects for **3** were larger in the case of AAA than in the case of LTL-A, reflecting a slightly higher affinity of **3** for AAA. In disaccharide **3** only trNOEs across the α(1→3)-glycosidic linkage could be employed to determine the bioactive conformation. The general strategy followed the examples described above and will therefore not be discussed in detail. It was found that two interglycosidic trNOEs, H1^F–H3^{GN} and H1^F–Nac^{GN}, were sufficient to analyze the conformation of **3** bound to the lectins AAA and LTL-A. In the case of AAA both trNOEs were observed, whereas for **3** bound to LTL-A only the trNOE H1^F–H3^{GN} was present. This indicated slightly different bioactive conformations of **3** when bound to AAA and LTL-A. Applying the trNOE H1^F–Nac^{GN} as a negative distance constraint led to the results shown in Table 5. Whereas AAA recognized the global minimum of disaccharide **3**, LTL-A slightly distorted the orientation of the α(1→3)-glycosidic linkage upon binding. Nevertheless, the conformation of **3** bound to LTL-A is similar to the global minimum, too.

For disaccharide **3** bound to AAA, also intermolecular trNOEs were observed (Figure 6). Usually, these effects are rather small. Therefore, the observation of intermolecular trNOEs has not been described often, although in principle they are useful for the conformational analysis of bound ligands.¹² In this case trNOEs were observed for the protons H4^F and H6^F. As shown in Figure 6 protons of aromatic amino acids of AAA were responsible for the effects observed. This observation suggested that the fucose residue, in particular the protons H4^F and H6^F, was in close contact with the lectin binding site.

Line Broadening Effects upon Binding of Saccharides 1–3 in the Presence of AAA and LTL-A. With the exception of

Table 4. Dihedral Angles for the Global and Local Minima of sLe^x^a

min	NeuNAc(2→3)Gal ϕ/ψ (deg)	Gal(1→4)GlcNAc ϕ/ψ (deg)	Fuc(1→3)GlcNAc ϕ/ψ (deg)	rel energy (kcal/mol)
aA	-68/-3	49/12	51/23	0.0
bA	-171/-8	52/10	50/24	1.3
cA	62/-10	52/11	50/24	6.2
aB	-61/-4	67/17	-25/-28	7.7
aD	-62/-4	40/23	7/5	7.9

^a Capital letters denote the conformation of the Le^x core structure (cf. Table 1). Small letters indicate the conformation at the $\alpha(2\rightarrow3)$ -glycosidic linkage between Neu5Ac and Gal. Conformation aD is bound by AAA.

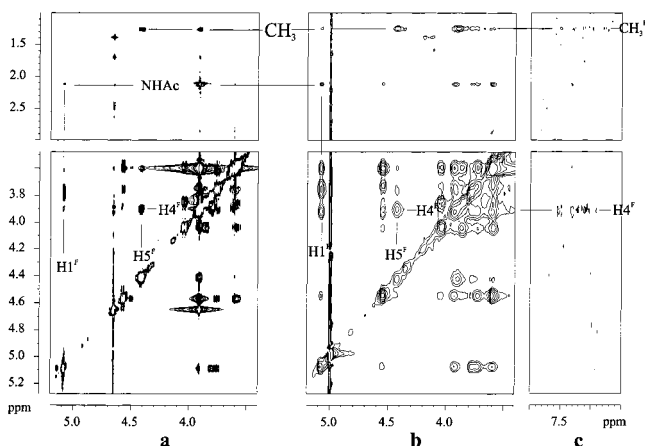


Figure 6. (a) NOESY and (b) trNOESY spectra of disaccharide **3** bound to AAA. Panel c shows a part of the trNOESY spectrum where intermolecular trNOEs to protons of aromatic amino acid side chains are observed. The mixing times were 900 ms for the NOESY and 200 ms for the trNOESY spectrum. The protons H^{4F} and H^{6F} from the fucose residue display intermolecular trNOEs to the protein.

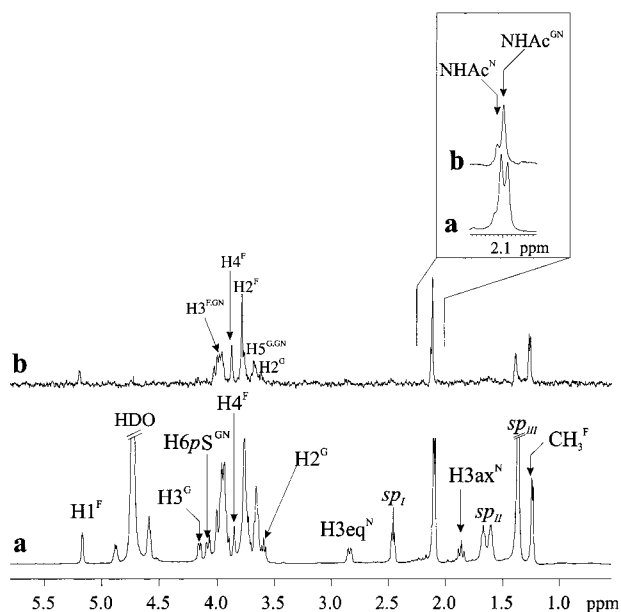


Figure 7. (a) ¹H NMR and (b) STD NMR spectra of **1** in the presence of AAA (molecular ratio 1:100). For the STD NMR spectrum the protein was saturated with 40 selective Gaussian-shaped pulses (50 ms each) resulting in a total saturation time of ~2 s (on-resonance 8.80 ppm, off-resonance 40.00 ppm). The residual water signal was reduced using the WATERGATE sequence. STD signals from the fucose residue are most prominent. STD signals from the Neu5Ac residue and the spacer give the weakest response.

sLe^x in the presence of LTL-A, where no line broadening was observed, significant broadening of ¹H NMR resonance lines was observed for all three saccharides, sLe^x (**1**), Le^x (**2**), and disaccharide **3** (see Supporting Information) in the presence of

AAA or LTL-A. In each case the lines of the fucose residue showed the strongest effects, indicating that the fucose was in close contact with the lectin binding site. At similar lectin-to-ligand ratios the different amounts of line broadening allowed one to estimate relative binding affinities of the saccharides. In general, line broadening was more pronounced for AAA than for LTL-A, and for both lectins the largest effects were observed for disaccharide **3**, followed by Le^x. Weakest effects were observed for sLe^x. This suggested that compared to LTL-A, AAA had a higher binding affinity to all three saccharides. Likewise, from the saccharides investigated, disaccharide **3** should have the highest binding affinity to both lectins.

Epitope Mapping of Saccharides 1–3 Bound to AAA or LTL-A with STD NMR. To map the binding epitope of the saccharides bound to the lectins we performed STD NMR experiments.¹³ Except for sLe^x in the presence of LTL-A, STD effects were observed for all saccharides complexed with AAA or LTL-A. In general, it was found that the fucose residues gave the largest STD signals, indicating that this residue was chiefly responsible for the binding reaction. We will only present one example of sLe^x bound to AAA because the results for the other saccharide–lectin complexes are analogous.

Figures 7 and 8 show 1D STD NMR spectra and a STD TOCSY spectrum of sLe^x bound to AAA, respectively. It is immediately obvious that the fucose residue leads to the most prominent STD signals. For instance, at the contour level chosen for the STD TOCSY in Figure 8 only fucose signals are visible. From the 1D STD spectra it can easily be seen that from the two *N*-acetyl groups present in sLe^x one of the GlcNAc residues is giving a larger STD response and, therefore, is in more intimate contact with the lectin binding site. This *N*-acetyl group is adjacent to the $\alpha(1\rightarrow3)$ -glycosidic linkage, suggesting that the molecular topology in the vicinity of the glycosidic linkage is important for the binding specificity.

The cross-peaks in the STD TOCSY spectrum were integrated and referenced to the off-resonance TOCSY spectrum to quantitate the binding epitope of sLe^x.^{13a} The reference cross-peak was deliberately set at 100%. A cross-peak in the STD TOCSY spectrum should reflect the averaged STD effects of the two protons involved, and therefore, cross-peaks should be symmetrical. In practice, the STD TOCSY cross-peaks were not symmetrical (Figure 9). For instance, the cross-peaks H^{5F}–H^{4F} differed significantly in their intensities above and below the diagonal. In this case, the difference was attributed to the low intensity of the cross-peaks (small *J* coupling between H^{5F} and H^{4F}) which generated a large error. A general explanation of the effect is not straightforward, and no attempt for an

(12) (a) Krishna, N. R.; Moseley, H. N. B. In *Biological Magnetic Resonance*; Krishna, N. R., Berliner, L. J., Eds.; Kluwer Academic/Plenum Press: New York, 1999; Vol. 17, pp 223–307. (b) Moseley, H. N.; Lee, W.; Arrowsmith, C. H.; Krishna, N. R. *Biochemistry* **1997**, *36*, 5293–5299.

(13) (a) Mayer, M.; Meyer, B. *J. Am. Chem. Soc.* **2001**, *123*, 6108–6117. (b) Vogtherr, M.; Peters, T. *J. Am. Chem. Soc.* **2000**, *122*, 6093–6099. (c) Klein, J.; Meinecke, R.; Mayer, M.; Meyer, B. *J. Am. Chem. Soc.* **1999**, *121*, 5336–5337. (d) Mayer, M.; Meyer, B. *Angew. Chem.* **1999**, *11*, 1902–1906; *Angew. Chem., Int. Ed. Engl.* **1999**, *38*, 1784–1788.

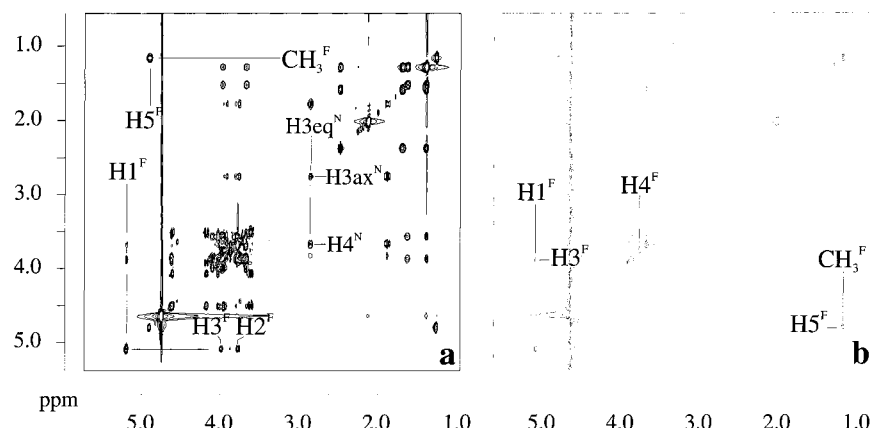


Figure 8. (a) TOCSY spectrum and (b) STD TOCSY spectrum of sLe^x (**1**) in the presence of AAA (molecular ratio 1:100). For the spin-lock period a MLEV17 sequence was used. The mixing time was 60 ms. Saturation of the protein was achieved by applying a cascade of 40 Gaussian pulses (50 ms each) used resulting in a total saturation time of ~2 s (on-resonance 8.80 ppm, off-resonance 40.00 ppm).

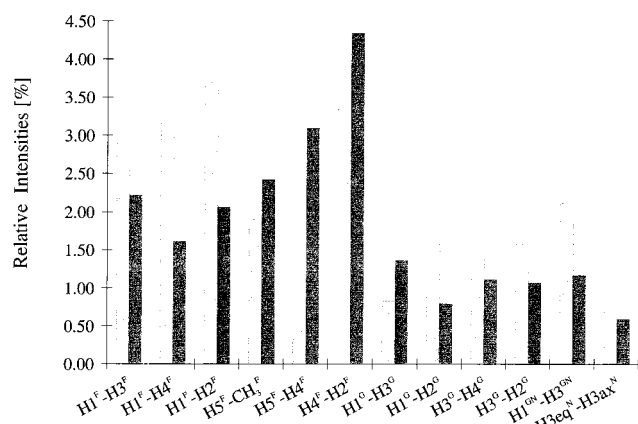


Figure 9. Relative intensities of cross-peaks in the STD TOCSY spectrum (cf. Figure 8) of sLe^x (**1**) in the presence of AAA. Each cross-peak is referenced to the corresponding cross-peak in the TOCSY spectrum (the off-resonance TOCSY was used as reference spectrum). Protons of the fucose residue receive the largest amount of saturation. Proton H4^F also shows an intermolecular trNOE to protons in an aromatic amino acid side chain (cf. Figure 6). Grey and black bars denote cross-peaks in F₁ and F₂, respectively.

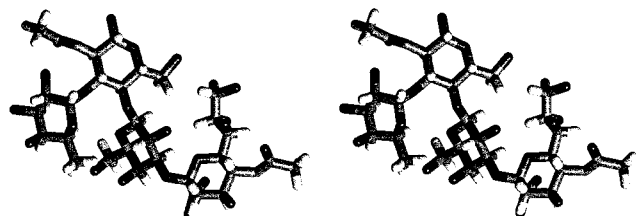


Figure 10. Bioactive conformation of sLe^x bound to AAA as a relaxed eye stereo representation (conformation aD in Table 4). It is obvious that the stacking interaction between the galactose and the fucose residue is absent (cf. also Figure 2). The neuramic acid orientation is very similar to the one found for sLe^x bound to E-selectin.

explanation will be made here. The diagram in Figure 9 summarizes the results of the cross-peak analysis. Although corresponding cross-peaks below and above the diagonal differed in size, several interesting conclusions were reached. It was observed that cross-peaks involving H4^F and H1^F gave the largest STD response. This was in accordance with the observation of intermolecular trNOEs for H4^F in disaccharide **3** (cf. discussion above) which suggested a close contact between H4^F and an aromatic amino acid of AAA. The analysis also showed that protons other than fucose protons were receiving

Table 5. Dihedral Angles for Disaccharide **3** from GEGOP Calculations^a

	ϕ/ψ (deg)	rel energy (kcal/mol)	H1 ^F -Nac ^{GN} (Å)
global min aq soln	49/16	0.0	3.4
+ AAA	49/16	0.0	3.4
+ LTL-A	44/5	0.3	4.0

^a Both lectins recognize conformations that are very similar to the global minimum (minimum A; cf. Table 1).

Table 6. K_D Values (μ M) from SPR Experiments^a

ligand	LTL-A	AAA
L-fucose	197	31
α -L-Fuc-(1 \rightarrow 3)- β -D-GlcNAc-OMe (3)	95	32
α -L-Fuc-(1 \rightarrow 4)- β -D-GlcNAc-OMe (5)	134	21
α -L-Fuc-(1 \rightarrow 2)- β -D-Gal-OMe (6)	58	19
α -L-Fuc-(1 \rightarrow 6)- β -D-GlcNAc-OMe (8) ^b	nd	33
Le ^x (2)	225	220
Le ^a (4)	1450	299
sLe ^x (1)	c	440

^a For details see Experimental Section. ^b Data are from ref 15. ^c No binding detected.

much less saturation from the protein during the STD experiment. Apart from the fucose signals, the cross-peak between H1^{GN} and H3^{GN} showed the largest intensity in the STD TOCSY spectrum, which was not surprising because H3^{GN} is located at the glycosidic linkage site. The weakest STD TOCSY cross-peaks were observed for the Neu5Ac protons indicating that this residue is not involved in the molecular recognition process to a significant extent.

SPR Measurements. The saccharides **1–3** were subjected to surface plasmon resonance measurements¹⁴ to determine dissociation constants K_D for the binding to LTL-A and AAA. Three other oligosaccharides, Le^a (**4**) (Lewis^a, β -D-Gal-(1 \rightarrow 3)-[α -L-Fuc-(1 \rightarrow 4)]- β -D-GlcNAc-OMe), α -L-Fuc-(1 \rightarrow 4)- β -D-GlcNAc-OMe (**5**), and α -L-Fuc-(1 \rightarrow 2)- β -D-Gal-OMe (**6**), as well as L-fucose (**7**), were also investigated. The lectins AAA and LTL-A were immobilized on a dextran chip, and the results are compiled in Table 6. The data were similar to K_D values determined previously for L-fucose and for the disaccharide α -L-Fuc-(1 \rightarrow 6)- β -D-GlcNAc-OMe (**8**).¹⁵ These data are also included in Table 6. In general, the experiments showed that AAA

(14) (a) Rich R. L.; Myszyka D. G. *Curr. Opin. Biotechnol.* **2000**, *11*, 54–61. (b) Morton, T. A.; Myszyka, D. G. *Methods Enzymol.* **1998**, *295*, 268–294.

(15) Weimar, T.; Haase, B.; Köhli, T. J. *Carbohydr. Chem.* **2000**, *19*, 1083–1089.

had a larger binding affinity than LTL-A to all saccharides. The binding affinity decreased with increasing complexity of the saccharide and was optimal for the disaccharides with the exception of disaccharide **8**, which had a lower binding affinity to AAA as compared to L-fucose (**7**). Disaccharide **8** contained a flexible (1→6)-glycosidic linkage and was therefore different from the other disaccharides.

Discussion

trNOE and STD NMR experiments were employed as key techniques to characterize the binding of the oligosaccharides **1–3** to the fucose recognizing lectins AAA and LTL-A with atomic resolution. For the trNOE experiments protein-mediated spin diffusion was largely excluded by performing trROESY and QUIET-trNOESY control experiments. It should be noted at this point that there is still the possibility of protein leakage that is not removed by these experiments and leads to slightly expanded structures for bound ligands. A more detailed discussion is found in ref 12. Dissociation constants K_D for the complexes were determined by utilizing SPR experiments furnishing a comprehensive model for the molecular recognition reactions between the oligosaccharides and the lectins.

The bioactive conformations of the oligosaccharides **1–3** bound to the lectins AAA and LTL-A (cf. Figures 2 and 10) were derived from trNOE experiments. It is observed that Le^x (**2**) and sLe^x (**1**) bind to the lectins in conformations where the $\alpha(1\rightarrow3)$ -fucosidic linkage is severely distorted compared to the global minimum conformation (Tables 1 and 4). The dihedral angles ϕ and ψ in the bioactive conformations of **1** and **2** are negative or very close to zero, and thus, do not obey the *exo*-anomeric effect. The reason for this distortion becomes clear when inspecting the molecular model of the global minimum conformation A and the bound conformations of Le^x and sLe^x (conformations B and D, respectively). Both lectins, AAA and LTL-A, are fucose-recognizing lectins. In the global minimum conformation A of Le^x or sLe^x a stacking of the galactose and fucose residues prohibits an interaction of the hydrophobic side of fucose with the lectin binding site (Figures 2 and 10). To come into contact with the protein surface, the fucose residue has to be reoriented. Obviously, this reorientation takes place around the $\alpha(1\rightarrow3)$ -glycosidic linkage. Other distortions of Le^x or sLe^x , e.g. at the $\beta(1\rightarrow4)$ -glycosidic linkage, apparently require more energy. This is in accordance with MMC simulations of Le^x that yield conformer B as local minimum, albeit with a high relative potential energy. The observation of a weak NOE between H1^F and H2^G for free Le^x (**2**) suggests that the local minimum B is populated in aqueous solution to a small extent (probably less than 1%). Other authors have already predicted the existence of this conformational family, but so far direct experimental evidence was lacking.⁹

Distortions of glycosidic linkages upon binding to proteins have already been observed before,^{11,16} but it is difficult to estimate the energy that is required to allow the binding of such distorted conformations. For the contribution of the *exo*-anomeric effect to the stabilization of glycosidic linkage orientations experimental values have been published recently and suggest values of at least ca. 2 kcal/mol.¹⁷ To compare with, the K_D values determined in this work (Table 6) allow one to give a crude estimate of the energy required for the distortion of the $\alpha(1\rightarrow3)$ -glycosidic linkage. Both lectins bind the disac-

charide **3** in a conformation that is close to the global minimum (Table 5). On the other hand, the Le^x trisaccharide **2** is bound in a significantly altered conformation in both cases (Table 1). From Table 6 it is seen that K_D is ca. 2-fold higher for trisaccharide **2** than for disaccharide **3** in the case of LTL-A and ca. 7-fold higher in the case of AAA. This translates into differences of the total free energies of binding, $\Delta\Delta G$ of 1.7 and 4.8 kcal/mol, respectively. Therefore, we suggest that the energy to overcome the *exo*-anomeric effect significantly contributes to the overall binding energy in the case of the Le^x trisaccharide.

In the bioactive conformations B and D for Le^x and aD for sLe^x , respectively, the fucose residue is oriented such that no steric conflicts prohibit the insertion of the fucose residue into the lectin binding pocket (Figures 2 and 10). As a comparison, in the case of sLe^x binding to E-selectin, access of the protein to the fucose hydroxy groups 3-OH and 4-OH is required for complexation with a Ca^{2+} ion in the binding pocket.¹⁸ These hydroxy groups are well accessible in the global minimum conformation A at the $\alpha(1\rightarrow3)$ -glycosidic linkage. Therefore, in this case no distortion of the fucose glycosidic linkage is necessary for molecular recognition.

For the $\alpha(2\rightarrow3)$ -glycosidic linkage between Neu5Ac and Gal the bound conformation is very similar to the one that has been observed for sLe^x bound to E-selectin.⁶ Recently, an X-ray structure for E-selectin complexed with sLe^x was published.¹⁸ The data indicate the same gross conformational features for the bioactive conformation of sLe^x . Unfortunately, it is difficult to compare structural details because no dihedral angles for the glycosidic linkages were reported, and coordinates are not yet available from the protein data bank.

From the STD NMR experiments it is obvious that the lectins AAA and LTL-A provide a binding pocket that is tailored for the specific recognition of L-fucose since the fucose residue in the oligosaccharides **1–3** leads to the most intense STD signals. The glycosidic linkage to the fucose fine-tunes the recognition by the lectins. STD spectra of the saccharides **1–3** show significant signals for the protons at the fucosidic linkage indicating that this glycosidic linkage is also in contact with the protein binding site. It should be noted here that while in practice protons not showing STD effects are generally far away from the protein surface, they may still be making contact to a region of the protein that is devoid of protons. A comparison of K_D values derived from SPR experiments (Table 6) for several oligosaccharides binding to LTL-A and AAA reveals interesting correlations. In general, disaccharides bind better than L-fucose to both lectins. This correlates very well with the results from the STD NMR experiments. Disaccharide **8** which contains a flexible $\alpha(1\rightarrow6)$ -glycosidic linkage is an exception because it has a lower binding affinity toward AAA than L-fucose. This might be due to the flexibility of the $\alpha(1\rightarrow6)$ -glycosidic linkage which should be reduced in the bound state¹⁹ leading to a loss in conformational entropy and thus to a lower binding affinity.

Tri- and tetrasaccharides have a lower binding affinity for the lectins (Table 6), which is also reflected by less severe line broadening upon binding. LTL-A has greater steric demands on the ligand than AAA, as seen by a very large K_D value for

(16) (a) Espinosa, J. F.; Montero, E.; Vian, A.; García, J. L.; Dietrich, H.; Schmidt, R. R.; Martín-Lomas, M.; Imbert, A.; Canada, F. J.; Jiménez-Barbero, J. *J. Am. Chem. Soc.* **1998**, *120*, 1309–1318. (b) Milton, M. J.; Bundle, D. R. *J. Am. Chem. Soc.* **1998**, *120*, 10547–10548.

(17) (a) Asensio, J. L.; Canada, F. J.; Garcia-Herrero, A.; Murillo, M. T.; Fernandez, A.; Johns, B. A.; Kozak, J.; Zhu, Z.; Johnson, C. R.; Jimenez-Barbero, J. *J. Am. Chem. Soc.* **2000**, *121*, 11318–11329. (b) Asensio, J. L.; Canada, F. J.; Cheng, X.; Khan, N.; Mootoo, D. R.; Jimenez-Barbero, J. *Chem. Eur. J.* **2000**, *6*, 1035–1041.

(18) Somers, W. S.; Tang, J.; Shaw, G. D.; Camphausen, R. T. *Cell* **2000**, *103*, 467–479.

(19) Weimar, T.; Peters, T. *Angew. Chem., Int. Ed. Engl.* **1994**, *33*, 88–91.

the Le^a trisaccharide **4** and no detectable binding for tetrasaccharide sLe^x (**1**).

Fine details of molecular recognition for disaccharide **3** as deduced from trNOE experiments are also in excellent agreement with the data from SPR measurements. It is observed that the glycosidic linkage conformation of **3** is slightly distorted upon binding to LTL-A, whereas the global minimum conformation is recognized by AAA. This corresponds to a larger K_D value of **3** when binding to LTL-A (Table 6).

Conclusions

STD NMR and trNOESY experiments in conjunction with SPR measurements yield models that describe the molecular recognition of oligosaccharides by corresponding lectins at atomic resolution. Bioactive conformations and binding epitopes of the oligosaccharides **1–3** bound to AAA or LTL-A were obtained. With SPR the binding specificity of these and other oligosaccharides was determined quantitatively. In concert with the NMR data this provides a detailed structure activity relationship.

It is interesting to note that previously the Le^x trisaccharide had always been described as quite rigid. For instance, upon binding to E-selectin sLe^x does not significantly alter the conformation of the Le^x core; only for the $\alpha(2\rightarrow3)$ glycosidic linkage is one of the conformational families present in solution selected. In contrast, our study shows that upon binding to particular protein receptors the orientation of the $\alpha(1\rightarrow3)$ glycosidic linkage in Le^x may well change. Certainly, this may also be the case for carbohydrate recognizing proteins in the human body and may well be linked to pathogenic processes such as metastasis.

Experimental Section

Purification of LTL-A. LTL-A was purified according to Yariv et al.^{4f} Seeds of *Lotus tetragonolobus* were purchased from Schumacher Inc. Dry *Lotus tetragonolobus* seeds (50 g) were grounded in a blender, and the powder was soaked in 2 L of 20 mM sodium phosphate buffer containing 0.85% sodium chloride (pH 6.8) at 4 °C. The crude extract was centrifuged, and the supernatant was fractionated by addition of solid ammonium sulfate (30% saturation). The suspension was centrifuged at 8500 rpm for 30 min at 4 °C. Ammonium sulfate (60% saturation) was added to the supernatant, and the solution was left overnight at 4 °C. The precipitate was centrifuged, and the pellet was suspended in 500 mL of 50 mM sodium phosphate buffer (pH 6.8). Dialysis (overnight) against 50 mM sodium phosphate buffer and subsequent centrifugation led to a supernatant solution that was applied to a column (2 × 10 cm) of L-fucosyl-4B-Sepharose (Sigma). The column was washed extensively with 50 mM sodium phosphate buffer (pH 6.8), and the bound lectin was eluted with 40 mM L-fucose in the same buffer. The lectin which was eluted in a single peak was dialyzed against 50 mM ammonium hydrogen carbonate solution and then lyophilized. The lyophilate was resuspended in 2–3 mL of 10 mM sodium phosphate buffer (pH 7.6) and then applied to a DEAE-cellulose (Merck) column (1.6 × 30 cm) running in the same buffer. Isolectin A was eluted with the buffer, whereas isolectins B and C were eluted with 200 mM sodium chloride solution. Subsequent dialysis against 50 mM ammonium hydrogen carbonate solution, and lyophilization yielded LTL-A that migrated as a homogeneous molecular species with a molecular weight of approximately 27 kDa on SDS-PAGE.

NMR Sample Preparation for the Free Ligands. The Lewis^x-trisaccharide β -D-Gal-(1→4)[α -L-Fuc-(1→3)]- β -D-GlcNAc-OMe (**2**) (MW 554.54) was purchased from Toronto Research Chemicals (Toronto, Canada). For NMR experiments 5.0 mg (9.0 μ mol) of **2** was used. The sialyl Lewis^x-tetrasaccharide α -D-Neu5Ac-(2→3)- β -D-Gal-(1→4)-[α -L-Fuc(1→3)]- β -D-GlcNAc-O(CH₂)₈COOMe (**1**) (MW 1012.99) was a generous gift from Prof. B. Ernst, University of Basel, Basel, Switzerland. For NMR experiments 5 mg (4.9 μ mol) of **1** was dissolved

in D₂O. Disaccharide **3**, α -L-Fuc-(1→3)- β -D-GlcNAc-OMe (MW 381.54), was synthesized. For NMR experiments 2 mg (5.24 μ mol) of **3** was used. For the sample with deuterated disaccharide **3a** (MW 384.54), 4.7 mg (12.23 μ mol) was used. All compounds were lyophilized twice from 1.0 mL of D₂O (99.9% D, Aldrich) and were finally dissolved in 500 μ L of D₂O (99.998% D, Aldrich).

NMR Sample Preparation for Ligands Complexed with LTL-A. Only the isolectin LTL-A (pI 7.1) was used for the NMR experiments. Lectin concentrations were determined by UV absorption at 280 nm. LTL-A was transferred into 1.2 mL deuterated imidazole/D₂O buffer (7.5 mM, 0.1 mM CaCl₂, pH 7.4) and was then lyophilized. The sample was lyophilized twice from 1.0 mL of D₂O (99.9% D) and was finally dissolved in 600 μ L of D₂O (99.998% D, Sigma). The final concentration of imidazole was 15 mM, and the concentration of CaCl₂ was 0.2 mM. The sample contained 2.9 mg (24 nmol, corresponding to 96 nmol of binding sites) of LTL-A and 0.4 mg (718 nmol) of compound **2**, corresponding to a protein-binding site concentration of 0.16 mM and a ligand concentration of 1.19 mM. The molar ratio of saccharide **2** to binding sites was therefore 1:7.5.

Samples of LTL-A and compounds **1** and **3** were prepared in a like manner. One sample contained 8.31 nmol of protein (33.25 nmol of binding sites) and 252 μ g (249 nmol) of compound **1**, corresponding to a concentration of binding sites of 0.055 mM and a ligand concentration of 0.413 mM resulting in a molar ratio of 1:7.5 of ligand molecules to binding sites. Another sample contained 3.2 mg of LTL-A (27 nmol, 107 nmol of binding sites) and 0.3 mg (802 nmol) of compound **3**. The binding sites concentration was 0.177 mM, and the ligand concentration was 1.32 mM resulting in a molar ratio of 1:7.5 of ligand molecules to binding sites.

NMR Sample Preparation for Ligands Complexed with *Aleuria aurantia* Agglutinin. All protein concentrations were determined by UV absorption. *A. aurantia* agglutinin was purchased from Vector Lab., Inc., CA. A 1.55 mg amount of AAA (21.52 nmol, 43.04 nmol of binding sites) and 0.4 mg (642 nmol) of Le^x (**2**) were dissolved in 500 μ L of deuterated phosphate buffer (10 mM sodium phosphate, 10 mM sodium chloride, pH 6.8) resulting in a protein binding site concentration of 86 μ M and a ligand concentration of 1.29 mM (molar ratio of ligand molecules to binding sites was 1:15). Two cycles of lyophilization from 1.0 mL of D₂O (99.98% D, Sigma) each followed. Finally, the sample was dissolved in 500 μ L of D₂O (99.998% D, Sigma).

Complexes of sLe^x (**1**) or disaccharide **3** with AAA were prepared in a like manner. The sample of sLe^x (**1**) complexed with AAA contained 1 mg of lectin (13.88 nmol, 27.76 nmol of binding sites) and 0.3 mg (346 nmol) of compound **1** resulting in a concentration of binding sites of 54 μ M and a ligand concentration of 0.675 mM (molar ratio of ligand molecules to binding sites of 1:12.5). For STD NMR experiments another sample with a concentration of binding sites of 54 μ M and a concentration of ligand molecules **1** of 5.4 mM was used (molar ratio of ligand molecules to binding sites 1:100). For the experiments on the complex of **3** with AAA a sample containing 2.8 mg of AAA (38.8 nmol, 77.8 nmol binding sites) and 0.4 mg (1.16 mmol) of compound **3** was prepared. The protein binding site concentration was 132 μ M, and the ligand concentration was 1.98 mM (molar ratio of ligand molecules to binding sites was 1:15).

NMR Experiments. All NMR experiments were performed on a Bruker Avance DRX 500 or 600 MHz spectrometer. The measurements were performed at 310 K without sample spinning using the HDO signal as internal reference (4.65 ppm at 310 K). Data acquisition and processing were performed with XWINNMR software (Bruker) running on Silicon Graphics Indy and O2 workstations. TrNOEs and NOEs were integrated with the program AURELIA (Bruker). ¹H and ¹³C chemical shifts assignments have previously been reported for **2** and **1**. Our assignments were in agreement with these reported data. 2D NOESY experiments experiments with **1–3** in aqueous solution were performed using TPPI. A total of 512 (t_1) × 2 K (t_2) data points were recorded. A total of 32 scans and 16 dummy scans were performed. The relaxation delay was set at 3.8 s, and values of 900 ms for **2**, 1 s for **1**, and 800 ms for **3** were chosen for the mixing time. Suppression of the residual HDO signal was achieved by presaturation with a weak rf field for 1s during the relaxation delay and during the mixing time. Unless otherwise stated 2D-trNOESY spectra were recorded with 512

increments in t_1 and 2 K data points in t_2 . The spectral width was 10 ppm in both dimensions. A spinlock pulse with a strength of 5 kHz and a duration of 10 ms was applied after the first 90° pulse to suppress protein ^1H NMR signals.²⁰ After 64 dummy scans, 16 scans were recorded per t_1 increment. The residual HDO signal was presaturated with a weak rf field during relaxation and mixing time. A gradient pulse (1 ms, 5 G/cm) at the end of the mixing time was applied to remove transverse magnetization. Mixing times of 80, 150, 250, 350, 450, and 600 ms were chosen to generate NOE buildup curves. To remove Hartmann–Hahn artifacts, 2D-trROESY experiments were performed as T-ROESY experiments²¹ with a phase-alternated 180° pulse to generate the spin-lock field. 2 K (t_2) \times 512 (t_1) data points were recorded. The carrier frequency of the spin-lock field was set at 2.89 ppm to further attenuate Hartman–Hahn transfer. The spin-lock field had a width of 2.7 kHz. The mixing time was 150 ms. A total of 16 scans were performed per t_1 increment with 32 dummy scans at the beginning. The HDO signal was suppressed by presaturation for 1 s during the relaxation delay. The total relaxation delay was 3.5 s. Prior to Fourier transformation the data matrix was zero-filled to yield a 2 K \times 1 K data matrix that was multiplied with a 90° phase-shifted squared sine-bell function in both dimensions. A spectral width of 10 ppm was used in both dimensions. 2D QUIET-trNOESY¹⁰ spectra were performed with a modified NOESY sequence.¹¹ After the first 90° degree pulse the protein signals were suppressed by a spin-lock field (5 kHz, 10 ms). In the middle of the mixing time a Gaussian Q3 cascade or an I-BURP pulse was used for the double selective inversion. The programs xShape and Mule (Bruker) were used to generate multiple selective pulse shapes. In general, the truncation level was 1% and 256 data points were used for the pulse generation. The inversion pulses were calibrated by adjusting to maximum intensity of the inverted region with a modified 1D-QUIET-trNOESY pulse sequence. A gradient pulse (1 ms, 5 G/cm) at the end of the mixing time was used to improve the spectra quality. The 512 \times 2 K data points were recorded, zero filled to 1 K \times 2 K, and multiplied with 90° phase-shifted squared sine-bell functions prior to Fourier transformation. The spectral width was 10 ppm in F_1 and F_2 . The mixing times were 150 ms. Zero-filling of the acquired data (512 t_1 values and 2 K data points in t_2) led to a final data matrix of 1 K \times 2 K ($F_1 \times F_2$) data points. The baseline was corrected in F_2 and F_1 (third-order polynomial) prior to integration of cross-peaks volumes.

For the saturation transfer difference experiments (STD) the protein was saturated on-resonance at 8.80 ppm (off-resonance 40.00 ppm) with a cascade of 40 selective Gaussian-shaped pulses (50 ms) resulting in total saturation time of 2 s.

STD TOCSY spectra were recorded with 512 increments and 16 or 32 transients using a MLEV-17 spin-lock field of 60 ms at 7.5 kHz. The relaxation delay was set at 1.2 s. Saturation transfer was achieved by using 40 selective Gaussian 270° pulses with a duration of 50 ms and a spacing of 10 ms. The protein envelope was irradiated at 8.80 ppm (on-resonance) and 40 ppm (off-resonance). Protein presaturation was applied for ca. 2 s. Subsequent subtraction of on- and off-resonance spectra was achieved via phase cycling.

Experimental NOE curves were fitted to a double exponential function, $f(t) = p_0(e^{-p_2 t})(1 - e^{-p_1 t})$, with p_0 , p_1 , and p_2 being adjustable parameters.¹¹ The initial slope was determined from the first derivative at time $t = 0$, $f'(0) = p_0 p_1$. From the initial slopes interproton distances r were obtained by employing the isolated spin pair approximation. Then, interproton distances obtained from experimental trNOE or QUIET-trNOE curves were translated into distance constraints by assuming a rather generous experimental error of $\pm 20\%$. This procedure yields upper and lower distance bounds.¹¹ Interglycosidic trNOEs that were not observed for the complex were translated into negative distance constraints, with a corresponding minimum distance of 4.0 Å. The

distance constraints matrix was subsequently applied as a filter to MMC simulations to extract conformations obeying the distance constraints.

Computational Procedures. MMC simulations, calculation of low-energy conformations, and population distributions were performed by utilizing the GEGOP program.^{8b} Dihedral angles ϕ and ψ at the glycosidic linkages were defined as follows: $\phi = \text{H1-C1-O1-Cx}$ (for Neu5Ac: C1-C2-O2-Cx); $\psi = \text{C1-O1-Cx-Hx}$ (for Neu5Ac: C2-O2-Cx-Hx); $\omega = \text{O5-C5-C6-O6}$ (for Neu5Ac corresponding designations were used to indicate the orientation of the side chain) (x being the aglyconic linkage site). Glycosidic bond angles were free to rotate during the simulations, whereas pyranose rings were treated as rigid units in the $^4\text{C}_1$ conformation ($^1\text{C}_4$ conformation for Neu5Ac and Fuc). MMC simulations were carried out on a Silicon Graphics O2 R10000 workstation with 2×10^6 macro steps each and temperature parameters set at 600 and 2000 K for **1**. A total of 5×10^6 macro steps and a temperature parameter of 2000 K were used for **2** as this has been discussed in detail previously.

SPR Experiments. Lewis^a-trisaccharide β -D-Gal-(1 \rightarrow 3)[α -L-Fuc-(1 \rightarrow 4)]- β -D-GlcNAc-OMe (**4**) (MW 554.54) was purchased from Toronto Research Chemicals (Toronto, Canada). Disaccharides **5** and **6** were synthesized according to published protocols. All SPR experiments were performed with a Biacore 3000 instrument (Biacore AB, Uppsala, Sweden) at 25 °C using original Biacore HBS-EP buffer (10 mM Hepes, 150 mM NaCl, 0.005% polysorbate, 3 mM EDTA, pH 7.4) and a flow rate of 10 $\mu\text{L}/\text{min}$. The carboxylated dextran matrix of a CM5-chip was activated with an EDC/NHS solution (1-ethyl-3-(3-(dimethylamino)propyl)carbodiimide, *N*-hydroxysuccinimide) for 10–20 min until the SPR signal increased 200–300 resonance units (RU). Both lectins were injected in immobilization buffer ($\sim 10 \mu\text{g}/\text{mL}$, 10 mM sodium acetate, pH 5.0) to reach levels of 4000–6000 RU for each lectin. To stop the immobilization, all activated flow cells were deactivated with a solution of ethanolamine (1 M) for 15 min. Carbohydrate solutions (concentrations between 1 μM and 10 mM) in buffer were injected for 2 min into the flow cells using the kinject mode. The equilibrium response (after subtraction from the response of the reference surface) of each experiment was used to create saturation curves of analyte binding which were fitted to a 1:1 steady-state affinity model by employing the Biaevaluation software 3.0 (Biacore AB, Uppsala, Sweden).

Acknowledgment. This work was supported by the DFG (Teilprojekt B3 of SFB 470) and the BMBF (FKZ 031161). Financial support from the Verband der Chemischen Industrie is gratefully acknowledged. We thank Prof. B. Ernst for generous gift of the sLe^x sample. We thank Prof. E. Rietschel and PD Dr. U. Zähringer for generous access to the 600 MHz NMR in the Research Center Borstel. We also thank Drs. T. Keller and G. Wolff, Bruker Analytik GmbH, Rheinstetten, Germany, for continuing support. Finally, we thank S. Hengst, H. Kässner, T. Köhli, and W. Hellebrandt for technical assistance.

Supporting Information Available: Tables with chemical shift values of compounds **1–3**, three figures with expansions from trNOESY and trROESY spectra of Le^x in the presence of AAA and LTL-A, QUIET-trNOE curves of Le^x in the presence of AAA and LTL-A, ^1H NMR spectra of Le^x in the presence of AAA and LTL-A showing the effects of line broadening, and pulse programs for the 1D STD and the STD TOCSY experiments (for Bruker instruments). This material is available free of charge via the Internet at <http://pubs.acs.org>.

JA011156H

(20) Scherf, T.; Anglister, J. *Biophys. J.* **1993**, *64*, 754–761.

(21) Hwang, T.-L.; Shaka, A. J. *J. Am. Chem. Soc.* **1992**, *114*, 3157–3159.